Zhang et al. *Zool. Res.* 2022, 43(4): 600−603
https://doi.org/10.24272/j.issn.2095-8137.2022.037

ZR | Zoological Research

Letter to the editor Open Access

Dynamic transcriptional atlas of male germ cells during porcine puberty

DEAR EDITOR,

Spermatogenesis is the process by which male gametes are formed from spermatogonial stem cells (SSCs) and it is essential for the reliable transmission of genetic information between generations. After birth, prospermatogonia (ProSG) give rise to SSCs. While mouse spermatogenesis is relatively well studied, we are only just beginning to unravel this process in larger animals. Here, we analyzed key developmental transitions and differentiation trajectories by profiling neonatal, juvenile, and adult testes through single-cell sequencing (scRNA-seq). We found that SSCs were established at 30 days old, and that CDH1 was a novel cell surface marker for porcine ProSG and undifferentiated spermatogonia. In addition, integrated analysis revealed similarities between pig and human spermatogenesis. This study is the first to analyze the transcriptome of male germ cells during porcine testicular development through scRNA-seq, and further document the development and classification of porcine germ cells. This study advances our understanding of the timing of porcine testicular development and provides a foundational data resource with multiple modalities of analyses.

In mice, primary transitional prospermatogonia (T1-ProSG) are mitotically quiescent cells and begin to convert into secondary transitional (T2)-ProSG at postnatal day 1, which then resume proliferation and give rise to SSCs. T2-ProSG generate the “first wave of spermatogenesis” (Tan et al., 2020). Subsequently, self-renewing SSCs commence differentiation and produce successive and continuous waves of gametogenesis from 2–3 weeks after birth.

However, porcine ProSG do not generate the equivalent “first wave” of spermatogenesis, and proliferate continuously after birth, albeit at a different growth rate. Porcine ProSG migrate to the basement membrane of the seminiferous tubules and differentiate into SSCs during the first three months of birth (Tan et al., 2020). Furthermore, SSC markers are not the same between pigs and rodent models (Park et al., 2019; Zhang et al., 2020). Therefore, the mechanisms regulating the differentiation of porcine ProSG and SSC are not fully understood, and a dynamic transcriptional germ cell atlas of testicular development is not yet available.

In this study, we profiled 9 307 single-cell transcriptomes from the whole-testes of one infant (7 days old (D7)) and three juvenile (30, 60, and 90 days old (D30, D60, and D90, respectively)) Guanzhong black pigs for comparison with our recently published adult (150 days old (D150)) data (Zhang et al., 2021). Histological examination was conducted to explore the changes in morphology and complete timeline of porcine germ cell development, which revealed a clearly defined lamina and lumen across the tubules of the D90 and D150 samples (Figure 1A). ProSG and spermatogonia were detected before D90, and spermatocytes and a lower proportion of spermatids began to appear at D90.

To minimize batch effects, the mutual nearest neighbor (MNN) approach was used to integrate all scRNA-seq libraries. Using the Leiden algorithm and t-distributed stochastic neighbor embedding (t-SNE), 41 cell clusters were identified. The clusters were then differentiated by known markers (e.g., *DDX4*, *UCHL1*, *SYCP3*, and *TNP2*) (Supplementary Figure S1A–E) into three major germ cell types, i.e., ProSG & spermatogonia, spermatocytes, and spermatids (Figure 1B). The marker genes used to classify the germ cell subgroups were as follows: ProSG & spermatogonia (*UCHL1* and *KIT*), spermatocytes (*DMC1* and *PIWIL1*), and spermatids (*TNP1* and *PRM1*) (Supplementary Figure S1F).

To investigate the classification and transcriptomic features of porcine ProSG and spermatogonia, re-clustering analysis was conducted on the ProSG & spermatogonia cluster (Supplementary Figure S2A), with 18 cell clusters identified (Supplementary Figure S2B). Clustering analysis revealed nine cell types based on well-known markers of ProSG and

Received: 19 April 2022; Accepted: 04 June 2022; Online: 04 June 2022

Foundation items: This work was supported by the Shaanxi Science and Technology Department (2020NY-003) to T.Z. and City-University Joint Research Project for Qinba State Key Laboratory of Biological Resources and Environment

spermatogonia (Figure 1C, D). Two types of ProSG were identified (T1-ProSG and T2-ProSG). *PIWIL4* and *SOX17* were highly expressed in T1-ProSG, while *ETV4* and *PALLD* were highly expressed in T2-ProSG (Supplementary Figure S2C). These results are important for the future isolation, culture, and characterization of ProSG.

To explore changes in the ratios and differences in the proliferative capacities of T1-ProSG and T2-ProSG, immunofluorescence analysis was conducted using the ProSG marker *Dolichos biflorus* agglutinin (DBA) and cell proliferation marker proliferating cell nuclear antigen (PCNA) (Supplementary Figure S2D). Localization of DBA^+ cells was used to distinguish T1-ProSG (seminiferous tubule center) and T2-ProSG (seminiferous tubule periphery). Cell ratios of T1-ProSG and T2-ProSG were counted during testicular development (Figure 1E), which indicated that ProSG migration was asynchronous and the ratio of T2-ProSG gradually increased from birth to puberty. The proliferation of T1-ProSG, albeit at low rate, is consistent with previous histological examination of the relative number of germ cells (França et al., 2000). However, our findings are in contrast with previous rodent studies showing that ProSG are quiescent or degenerate massively after birth (Law & Oatley, 2020). The proliferative capacity of T2-ProSG was greater than that of T1-ProSG (Figure 1F). Between the two ProSG populations, 52 genes were up-regulated in T1-ProSG and 141 genes were up-regulated in T2-ProSG (Supplementary Figure S2E). Gene Ontology (GO) analysis indicated that cell-cycle activation was enriched in T2-ProSG (Supplementary Figure S2F). Genes up-regulated in T1-ProSG were involved in the cell migration pathway (*CAP1*, *CRK*, *JAK1*, *MESP2*, *CTTN*, *EZR*, and *IQGAP1*), suggesting that these cells exhibit a strong migration ability. Moreover, genes highly expressed in T2-ProSG were involved in the cell proliferation pathway (*PCNA*, *BUB1*, *CDK9*, *FGF8*, and *NEK2*) (Supplementary Figure S2G). Taken together, T1-ProSG and T2-ProSG were primarily found at D7 and D30, which advances our understanding of porcine male germ cell development at this stage, with a large reduction at D60 and rare detection at D90 (Supplementary Figure S2H). The ProSG began to transform into undifferentiated spermatogonia at D30, whereas differentiated spermatogonia began to appear at D60. Thus, it would be interesting to define T1- and T2-ProSG from a functional perspective in future work.

The cell-cycle score was calculated according to previously reported S and G2/M phase-specific genes (Nestorowa et al., 2016) (Supplementary Figure S3B). According to marker gene expression and cell-cycle analysis, 16 clusters were grouped into seven spermatogonia clusters, i.e., Undiff1, Undiff2, Undiff3, E-diff1, E-diff2, Mid-diff, and Late-diff (Figure 1C). SSC-associated marker genes, such as *ID4*, *PAX7*, *FGFR3*, *ZBTB16*, and *UCHL1*, were highly expressed in the Undiff1 subgroup. Interestingly, the expression levels of *PAX7* and *ID4*, which are SSC function markers, were reduced when Undiff1 transitioned to Undiff2 (Figure 1D). Furthermore, most germ cells in the Undiff1 subgroup were at the G1/G0 phase of the cell cycle (Supplementary Figure S3B), indicating quiescence. *ZBTB16* and *UCHL1* were highly expressed in the Undiff3 subgroup, while *ID4*, *PAX7*, *FGFR3*, and *ETV5* showed lower expression levels (Figure 1D). In rodents, SSCs and progenitor spermatogonia are comprised of As, Apr, and chains of Aal spermatogonia. SSCs are a subset of the As population and strongly express *ID4* (Fayomi & Orwig, 2018). Thus, we propose that Undiff1, Undiff2, and Undiff3 resemble As, Apr, and Aal spermatogonia, respectively. To the best of our knowledge, this is the first detailed classification of spermatogonia in large animals, thus providing a foundation for future characterization of spermatogonia.

Cells in the E-diff1 subgroup partially corresponded to Aal and A1–A4 spermatogonia, expressing differentiation markers (*KIT* and *DMRT1*) and proliferation marker (*PCNA*), with lower expression levels of SSC markers (*ZBTB16* and *ETV5*) (Figure 1D). E-diff2 corresponded to intermediate spermatogonia, with high expression of *KIT*, *CTCFL*, and *DMRT1*. Mid-diff corresponded to B spermatogonia, with high expression of *STRA8*, a marker of differentiating spermatogonia. Late-diff corresponded to pre-leptotene spermatocytes, with high expression of *SPO11*, *SYCP3*, and *REC8*.

The porcine spermatocytes were divided into Lep, Zyg, Pachy, and Dip & Sec subsets (Figure 1G; Supplementary Figure S4). Meiotic recombination-associated genes *REC8* and *SPO11* were highly expressed in Lep, whereas meiosis-specific cyclin gene *CCNA1* was highly expressed in Dip & Sec (Figure 1H). Spermatids were classified into nine subgroups, i.e., Early-RS1, Early-RS2, Early-RS3, Mid-RS, Late-RS, Early-ES, Mid-ES, Late-ES, and Sperm (Figure 1I; Supplementary Figure S4). *CD63* and *NME5* were highly expressed in Early-RS1-3, Mid-RS, and Late-RS. SPAG6 plays a critical role in acrosome formation and motility, whereas transition nuclear protein 1 and 2 (TNP1/2) are required for packaging and condensation of sperm chromatin. Here, *SPAG6* and *TNP1/2* were up-regulated when Late-RS transitioned to Early-ES and were further enhanced during differentiation. Following that, *PRM1* and *PRM2* showed high expression in the Sperm subgroup (Figure 1J). To elucidate the complete developmental trajectory of porcine spermatogenesis, we re-clustered the abovementioned annotated cell clusters (Figure 1C, G, I). Results showed a contiguous trajectory of porcine germ cell development, which allowed us to distinguish detailed changes that occurred during spermatogenesis (Figure 1K). Furthermore, pseudotime analysis was conducted to obtain an unbiased developmental trajectory of porcine spermatogenesis (Figure 1L). We thus proposed a model of porcine germ cell development (Figure 1O). Based on scRNA-seq analysis, partition-based graph abstraction (PAGA), and evidence from stage-specific genes, we reconstructed the developmental dynamics of porcine spermatogenesis and provided a molecular atlas of testicular development in pigs.

Interestingly, scRNA-seq analysis revealed that expression of *CDH1* was up-regulated in ProSG (Figure 1D). Double immunofluorescence staining for CDH1/DBA and CDH1/UCHL1 revealed that most CDH1-positive cells overlapped with DBA- and UCHL1-positive cells (Supplementary Figure S5), indicating that CDH1-positive cells represent a subset of ProSG and undifferentiated spermatogonia in pigs. Therefore, CDH1 could be beneficial

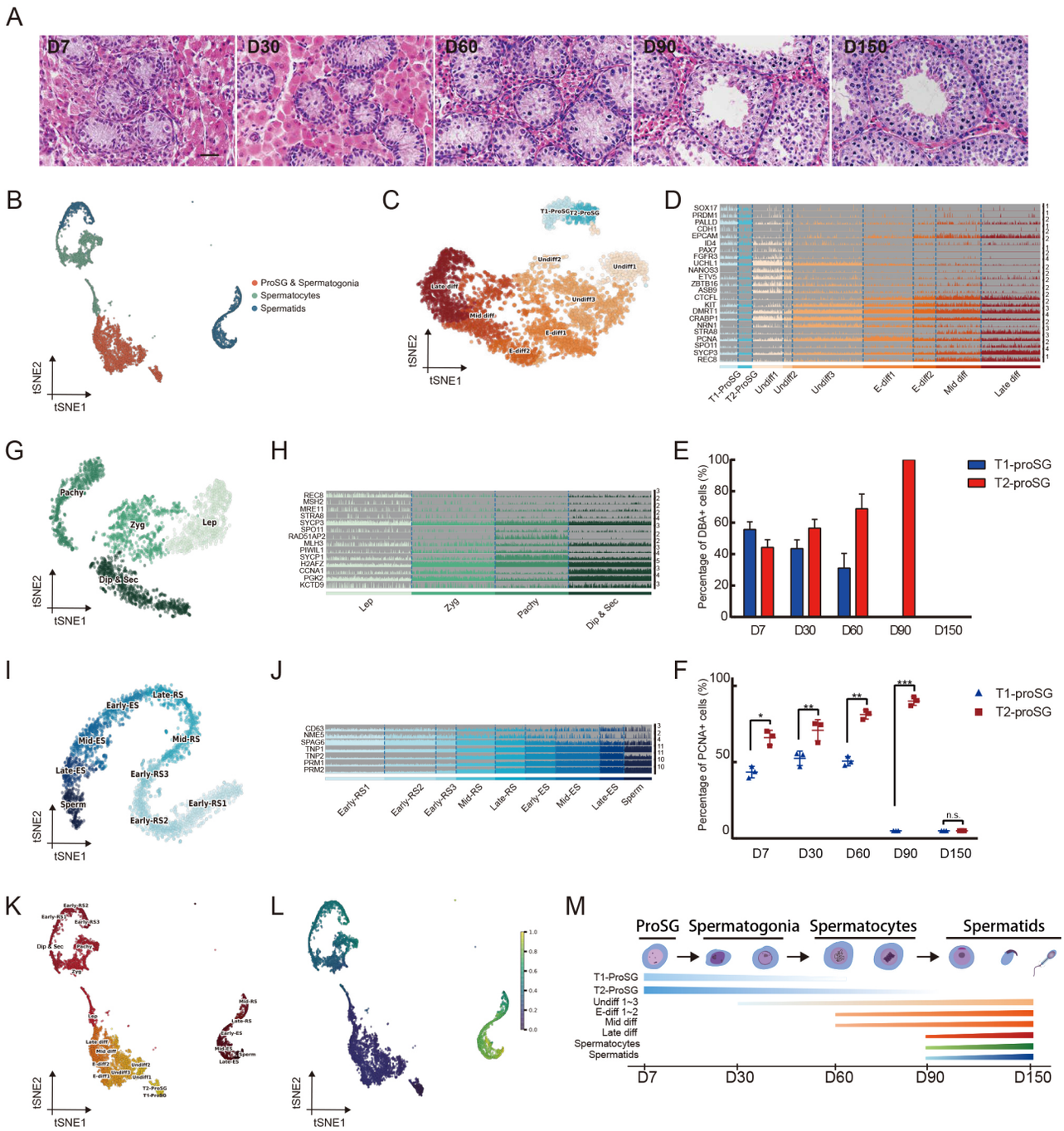

Figure 1 Single-cell RNA sequencing reveals atlas of germ cell development in porcine testes

A: Hematoxylin and eosin staining of testes from different ages revealed typical changes in morphology and cell types during puberty. Scale bar: 50 μm. B: t-SNE plot showing 9 307 germ cells (colored by three broad cell types: ProSG & spermatogonia, spermatocytes, and spermatids). C: t-SNE plot showing different substages of ProSG and spermatogonia (T1-ProSG, T2-ProSG, Undiff1, Undiff2, Undiff3, E-diff1, E-diif2, Mid diff, and Late diff). D: Expression of marker genes in ProSG and spermatogonia. Track-plot showing expression of genes at single-cell level, bars represent individual cells, colored according to cell type. Upper limits for y-axis are different for each track. E: Cell ratios of T1-ProSG and T2-ProSG during testicular development. F: Quantification of PCNA$^+$ T1-ProSG and T2-ProSG at different ages. Data are mean±standard deviation (*SD*) of independent experiments. *P*-value was calculated via Student's *t*-test. G: t-SNE plot showing spermatocyte cell types (Lep, Zyg, Pachy, Dip, & Sec). H: Track-plot showing marker gene expression of spermatocyte subgroups. I: t-SNE plot showing identified spermatid cell types (Early-RS1, Early-RS2, Early-RS3, Mid-RS, Late-RS, Early-ES, Mid-ES, Late-ES, and Sperm). J: Track-plot showing marker gene expression of spermatid subgroups. K: t-SNE plot showing overall classification of porcine germ cells. L: t-SNE plot showing developmental trajectories in pseudotime. M: Model of germ cell development during puberty, see text for details.

for sorting ProSG in neonate piglets, and potentially in other farm animals. Further studies are needed to uncover the role of *CDH1* during germ cell proliferation and differentiation.

During male meiosis, sex chromosomes undergo a tightly coordinated process known as meiotic sex chromosome inactivation (MSCI) (Turner, 2007). The inactivation and re-activation of sex chromosomes were evaluated by plotting the mean number of genes expressed from the sex chromosomes compared to all autosomes (Supplementary Figure S6A). Genes of the X chromosome declined sharply at the Zyg stage (Supplementary Figure S6B). *SCML2*, which is critical for heterochromatin organization in MSCI, was highly expressed in the Lep stage (Supplementary Figure S6C). In addition, gene repression during MSCI was mediated by H3K9me3, an epigenetic marker catalyzed by *SETDB1*. Analysis revealed that *SETDB1* was up-regulated in the spermatocytes (Supplementary Figure S6C), as verified by immunohistochemical assay (Supplementary Figure S6D).

Mammalian spermatogenesis is conserved among species and plays a crucial role in the transmission of genetic heritage. Pigs are important farm animals and one of the most important large animal models in biomedical research (Perleberg et al., 2018). In this study, comprehensive analysis revealed significant similarities in the spermatogenesis process between pigs and humans (Supplementary Figure S7). Our results and those of others (Fayomi & Orwig, 2018) suggest that many traits are conserved across species.

In summary, we revealed key developmental transitions in differentiation trajectories by profiling neonatal, juvenile, and adult testes using 10× Genomics scRNA-seq. We identified two types of prospermatogonia, seven types of spermatogonia, four types of spermatocytes, and nine types of spermatids. We also identified CDH1 as a novel cell surface marker for ProSG and undifferentiated spermatogonia in pigs. Furthermore, our integrated analyses highlighted the similarities in porcine and human spermatogenesis. This study advances our understanding of testicular development from birth to puberty and provides a foundational resource with multiple modalities of analysis.

DATA AVAILABILITY

Datasets generated in this study are available in the GSA at the National Genomics Data Center (CRA010185), NCBI Gene Expression Omnibus (GSE186479) and Science Data Bank (https://www.scidb.cn/en/s/Zb6bMz).

SUPPLEMENTARY DATA

Supplementary data to this article can be found online.

COMPETING INTERESTS

The authors declare that they have no competing interests.

AUTHORS' CONTRIBUTIONS

T.Z. and W.X.Z conceived and supervised the study. L.K.Z. analyzed the data. M.G., H.D.M., L.W., Y.Z., X.D.W., T.J.L., and H.Z.L. performed the experiments. T.Z. provided funding support. L.K.Z., H.D.M, T.Z., and W.X.Z. wrote the manuscript. All authors read and approved the final version of the manuscript.

Ling-Kai Zhang[1,2,#], Hai-Dong Ma[1,#], Ming Guo[2], Ling Wang[1], Yi Zheng[2], Xiao-Dong Wu[2], Tian-Jiao Li[2], Hong-Zhao Lu[1], Wen-Xian Zeng[2,*], Tao Zhang[1,*]

[1] *School of Biological Science and Engineering*, *Shaanxi University of Technology*, *Hanzhong*, *Shaanxi* 723001, *China*
[2] *College of Animal Science and Technology, Northwest A&F University, Yangling, Shaanxi 712100, China*
[#]Authors contributed equally to this work
*Corresponding authors, E-mail: zengwenxian2015@126.com; zhangtao780823@snut.edu.cn

REFERENCES

Fayomi AP, Orwig KE. 2018. Spermatogonial stem cells and spermatogenesis in mice, monkeys and men. *Stem Cell Research*, **29**: 207−214.

França LR, Silva VA Jr, Chiarini-Garcia H, Garcia SK, Debeljuk L. 2000. Cell proliferation and hormonal changes during postnatal development of the testis in the pig. *Biology of Reproduction*, **63**(6): 1629−1636.

Law NC, Oatley JM. 2020. Developmental underpinnings of spermatogonial stem cell establishment. *Andrology*, **8**(4): 852−861.

Nestorowa S, Hamey FK, Sala BP, Diamanti E, Shepherd M, Laurenti E, et al. 2016. A single-cell resolution map of mouse hematopoietic stem and progenitor cell differentiation. *Blood*, **128**(8): e20−e31.

Park HJ, Lee WY, Park C, Hong K, Song H. 2019. CD14 is a unique membrane marker of porcine spermatogonial stem cells, regulating their differentiation. *Scientific Reports*, **9**(1): 9980.

Perleberg C, Kind A, Schnieke A. 2018. Genetically engineered pigs as models for human disease. *Disease Models & Mechanisms*, **11**(1): dmm030783.

Tan K, Song HW, Wilkinson MF. 2020. Single-cell RNAseq analysis of testicular germ and somatic cell development during the perinatal period. *Development*, **147**(3): dev183251.

Turner JMA. 2007. Meiotic sex chromosome inactivation. *Development*, **134**(10): 1823−1831.

Zhang LK, Li FY, Lei PP, Guo M, Liu RF, Wang L, et al. 2021. Single-cell RNA-sequencing reveals the dynamic process and novel markers in porcine spermatogenesis. *Journal of Animal Science and Biotechnology*, **12**(1): 122.

Zhang PF, Li FY, Zhang LK, Lei PP, Zheng Y, Zeng WX. 2020. Stage-specific embryonic antigen 4 is a membrane marker for enrichment of porcine spermatogonial stem cells. *Andrology*, **8**(6): 1923−1934.

Supplementary Materials

Supplementary Materials and Methods

Animals and testis samples

Pig testis samples were acquired from Guanzhong black pigs aged 7, 30, 60, and 90 days old from the farm of Northwest A&F University (Yangling, China). All protocols and experiments were conducted in accordance with the Northwest A&F University Guide for the Care and Use of Laboratory Animals.

Generation of cell suspensions

Single-cell suspensions from seminiferous tubules were generated from the testes of Guanzhong black pigs using a two-step enzymatic digestion approach (Zhang et al., 2017). Briefly, testicular parenchyma was digested with 1 mg/mL Collagenase Type IV (Invitrogen) for 30 min at 34 °C and washed with Dulbecco's phosphate-buffered saline (DPBS; Invitrogen) to remove interstitial cells. The seminiferous tubules were then digested with 0.25% trypsin/EDTA (HyClone) for 5 min at 34 °C, followed by termination using 10% fetal bovine serum (FBS). Cell suspensions were filtered with 40 μm strainers, washed using DPBS with 0.5 mg/mL DNase I (Sigma) twice, then suspended in 1640/Dulbecco's Modified Eagles Medium (DMEM, HyClone) containing 5% FBS.

Hematoxylin and eosin staining

Testis tissues were fixed in Bouin's solution for 12 h before being transferred to 70% ethanol. The fixed tissues were embedded in paraffin and sectioned (5 μm thick). Coronal sections were de-paraffinized in xylene and re-hydrated in ethanol. The sections were then stained with hematoxylin for 5 min and incubated with 1% hydrochloric acid alcohol for 30 s. Slides were then rinsed in tap water for 10 min, followed by eosin staining for 2 min. Subsequently, sections were dehydrated and mounted with coverslips.

Single-cell testis transcriptomes using 10× Genomics Chromium platform

The cells were loaded into Chromium microfluidic chips using 10× Genomics 3' v3 chemistry to generate single-cell gel bead emulsions (GEMs) using the Chromium Controller according to the manufacturer's protocols. Libraries were sequenced on the Illumina NovaSeq6000 sequencing system by LC-Bio-Technology Co. Ltd., (Hangzhou, China). For gene expression data, FASTQ files were generated using CellRanger mkfastq. Alignment, filtering, and unique molecular identifier (UMI) counting were performed using CellRanger count. Sscrofa11.1 genome assembly/annotation was used as a reference. Further analysis used the UMI count tables.

Quality control, normalization, and batch-effect correction of scRNA-seq data

We filtered the data by retaining cells expressing >200 but <4 000 genes with <20% mitochondrial content and UMI counts between 2 000–100 000. In addition, we identified germ cells based on the well-established gene marker DDX4 and retained 9 307 germ cells for further analysis. We performed normalization by deconvolution with the scran package (Lun et al., 2016). We used the quickCluster function to pre-cluster cells following size factors. Expression values were scaled with the size factors, then log-transformed using the logNormCounts function. Unsupervised cell clustering and t-SNE analysis were performed on statistically significant principal

components. Batch effects were removed by the fast mutual nearest-neighbor correction (fastMNN) function in the bachelor R package (Haghverdi et al., 2018). Further downstream analysis was performed using the Scanpy (v1.7.1) tool, and SingleCellExperiment data were exported to anndata using the anndata2ri tool.

Cell cycle analysis

Cell cycle phase scores were calculated for each cell using the Scanpy function sc.tl.score_gene_cell_cycle. Genes associated with the S and G2M phases used in our datasets were from Tirosh et al. (2016).

Enrichment analysis

Metascape was used to perform enrichment analysis of marker genes. The pig genes were converted into orthologous human genes. Gene Ontology (GO) Biological Processes, Kyoto Encyclopedia of Genes and Genomes (KEGG) Pathways, Reactome Gene Sets, and CORUM were chosen as ontology sources. Based on membership similarities, the significantly enriched terms were grouped into clusters (P<0.01, minimum counts >3, and enrichment factor >1.5).

Iteration of human (GEO: GSE120508 and GSE134144) and pig datasets

Human testicular datasets from two independent studies using 10× Genomics sequencing (SRR9670686, SRR9670688, SRR9670690, SRR9670692, and SRR6860521) (Guo et al., 2018, 2020) were processed in a similar way to our porcine datasets. Raw human count matrices were filtered by retaining cells expressing >200 genes with <20% mitochondrial content. Human clusters were annotated using similar parameters.

Orthologous genes were obtained between humans and pigs using Ensembl. The one2one_ortholog-annotated orthologous genes in pigs were retained with the human reference. We identified 14 960 one-to-one orthologous genes for integration analysis. Pig-specific gene symbols were replaced by human orthologous gene symbols to combine the datasets.

Immunofluorescence assay

Sections were deparaffinized and rehydrated, with heat-mediated antigen retrieval then performed in 10 mM sodium citrate buffer. Sections were cooled for 30 min and blocked in 3% bovine serum albumin (BSA) for 2 h. The following primary antibodies were used: PCNA (1:200; Cell Signaling Technology, Catalog No. #2586), VASA (1:100; Abcam, Catalog No. ab13840), DBA (1:100; VECTOR), UCHL1 (1:200; Abcam, Catalog No. ab8189), CDH1 (1:200; Proteintech, Catalog No. 20874-1-AP), and SETDB1 (1:200; Cell Signaling Technology, Catalog No. #93212). Antigen reactions were conducted using the corresponding donkey anti-rabbit/mouse secondary antibodies (1:400; Alexa Fluor 488/594, Yeason) for 2 h at 4 °C in the dark. The sections were then incubated with 4’,6-diamidino-2-phenylindole (DAPI) (Bioworld Technology) to facilitate nuclear visualization.

REFERENCES

Ernst C, Eling N, Martinez-Jimenez CP, Marioni JC, Odom DT. 2019. Staged developmental mapping and X chromosome transcriptional dynamics during mouse spermatogenesis. *Nature Communications*, **10**(1): 1251.

Fayomi AP, Orwig KE. 2018. Spermatogonial stem cells and spermatogenesis in mice, monkeys and men. *Stem Cell Research*, **29**: 207–214.

França LR, Silva VA Jr, Chiarini-Garcia H, Garcia SK, Debeljuk L. 2000. Cell proliferation and hormonal changes during postnatal development of the testis in the pig. *Biology of Reproduction*, **63**(6): 1629–1636.

Guo JT, Grow EJ, Mlcochova H, Maher GJ, Lindskog C, Nie XC, et al. 2018. The adult human testis transcriptional cell atlas. *Cell Research*, **28**(12): 1141–1157.

Guo JT, Nie XC, Giebler M, Mlcochova H, Wang YQ, Grow EJ, et al. 2020. The dynamic transcriptional cell atlas of testis development during human puberty. *Cell Stem Cell*, **26**(2): 262–276.e4.

Haghverdi L, Lun ATL, Morgan MD, Marioni JC. 2018. Batch effects in single-cell RNA-sequencing data are corrected by matching mutual nearest neighbors. *Nature Biotechnology*, **36**(5): 421–427.

Hirota T, Blakeley P, Sangrithi MN, Mahadevaiah SK, Encheva V, Snijders AP, et al. 2018. SETDB1 Links the Meiotic DNA Damage Response to Sex Chromosome Silencing in Mice. *Developmental Cell*, **47**(5): 645-659 e646.

Law NC, Oatley JM. 2020. Developmental underpinnings of spermatogonial stem cell establishment. *Andrology*, **8**(4): 852–861.

Liu Y, Zhang L, Li W, Huang Q, Yuan S, Li Y, et al. 2019. The sperm-associated antigen 6 interactome and its role in spermatogenesis. *Reproduction*, **158**(2): 181-197.

Lun ATL, Bach K, Marioni JC. 2016. Pooling across cells to normalize single-cell RNA sequencing data with many zero counts. *Genome Biology*, **17**: 75.

Meistrich ML, Mohapatra B, Shirley CR, Zhao M. 2003. Roles of transition nuclear proteins in spermiogenesis. *Chromosoma*, **111**(8): 483-488.

Nestorowa S, Hamey FK, Sala BP, Diamanti E, Shepherd M, Laurenti E, et al. 2016. A single-cell resolution map of mouse hematopoietic stem and progenitor cell differentiation. *Blood*, **128**(8): e20–e31.

Park HJ, Lee WY, Park C, Hong K, Song H. 2019. CD14 is a unique membrane marker of porcine spermatogonial stem cells, regulating their differentiation. *Scientic Reports*, **9**(1): 9980.

Perleberg C, Kind A, Schnieke A. 2018. Genetically engineered pigs as models for human disease. *Disease Models & Mechanisms*, **11**(1): dmm030783.

Tan K, Song HW, Wilkinson MF. 2020. Single-cell RNAseq analysis of testicular germ and somatic cell development during the perinatal period. *Development*, **147**(3): dev183251.

Tirosh I, Izar B, Prakadan SM, Wadsworth II MH, Treacy D, Trombetta JJ, et al. 2016. Dissecting the multicellular ecosystem of metastatic melanoma by single-cell

RNA-seq. *Science*, **352**(6282): 189–196.

Turner JMA. 2007. Meiotic sex chromosome inactivation. *Development*, **134**(10): 1823–1831.

Zhang LK, Li FY, Lei PP, Guo M, Liu RF, Wang L, et al. 2021. Single-cell RNA-sequencing reveals the dynamic process and novel markers in porcine spermatogenesis. *Journal of Animal Science and Biotechnology*, **12**(1): 122.

Zhang PF, Chen XX, Zheng Y, Zhu JS, Qin YW, Lv YH, et al. 2017. Long-term propagation of porcine undifferentiated spermatogonia. *Stem Cells Development*, **26**(15): 1121–1131.

Zhang PF, Li FY, Zhang LK, Lei PP, Zheng Y, Zeng WX. 2020. Stage-specific embryonic antigen 4 is a membrane marker for enrichment of porcine spermatogonial stem cells. *Andrology*, **8**(6): 1923–1934.

Supplementary Figures

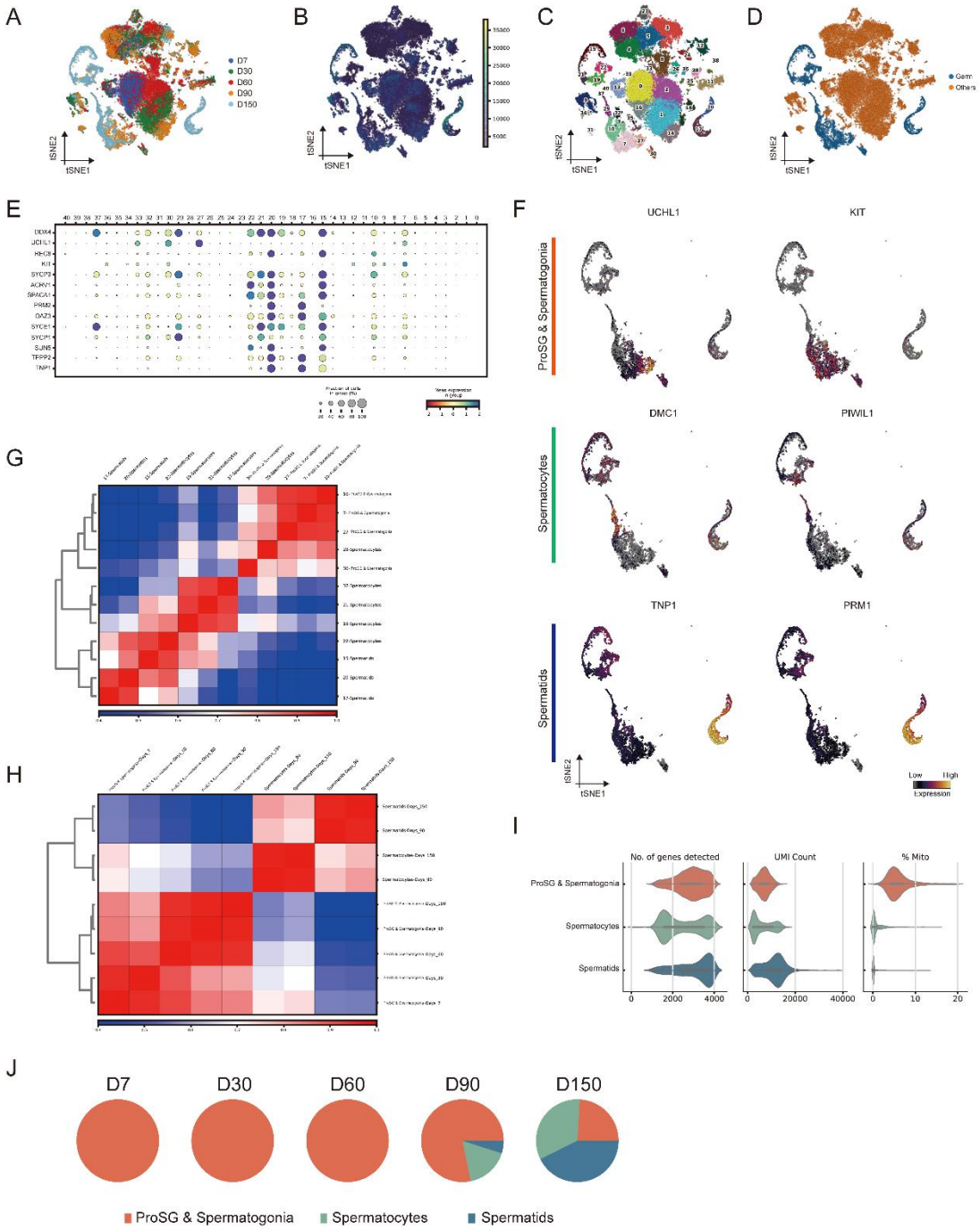

Supplementary Figure S1 Identification of major porcine germ cell types. A: t-SNE plot showing distribution of samples at different ages (D7, D30, D60, D90, and D150). B: t-SNE projection of per cell UMI counts. C: t-SNE plot showing unbiased cell clusters from all porcine testicular cells. D: t-SNE plot showing distribution of germ cells (expressing DDX4; blue) and other clusters (dark orange). E: Dot plot showing expression of marker genes in each Leiden cluster. F: Visualization of selected marker gene expression across all single cells in t-SNE plot. For each cell cluster, two cell markers are shown. G: Heatmap showing Pearson correlation

coefficients for germ cell clusters with hierarchical clustering. H: Within each broad cluster, Pearson correlation coefficients for cells derived from each pig sample were plotted in heatmap format. I: Distribution of cell attributes from each cell type in porcine dataset. J: Pie chart showing distribution of germ cells (ProSG & spermatogonia, spermatocytes, and spermatids) from different pig samples. Cell types are colored according to legend.

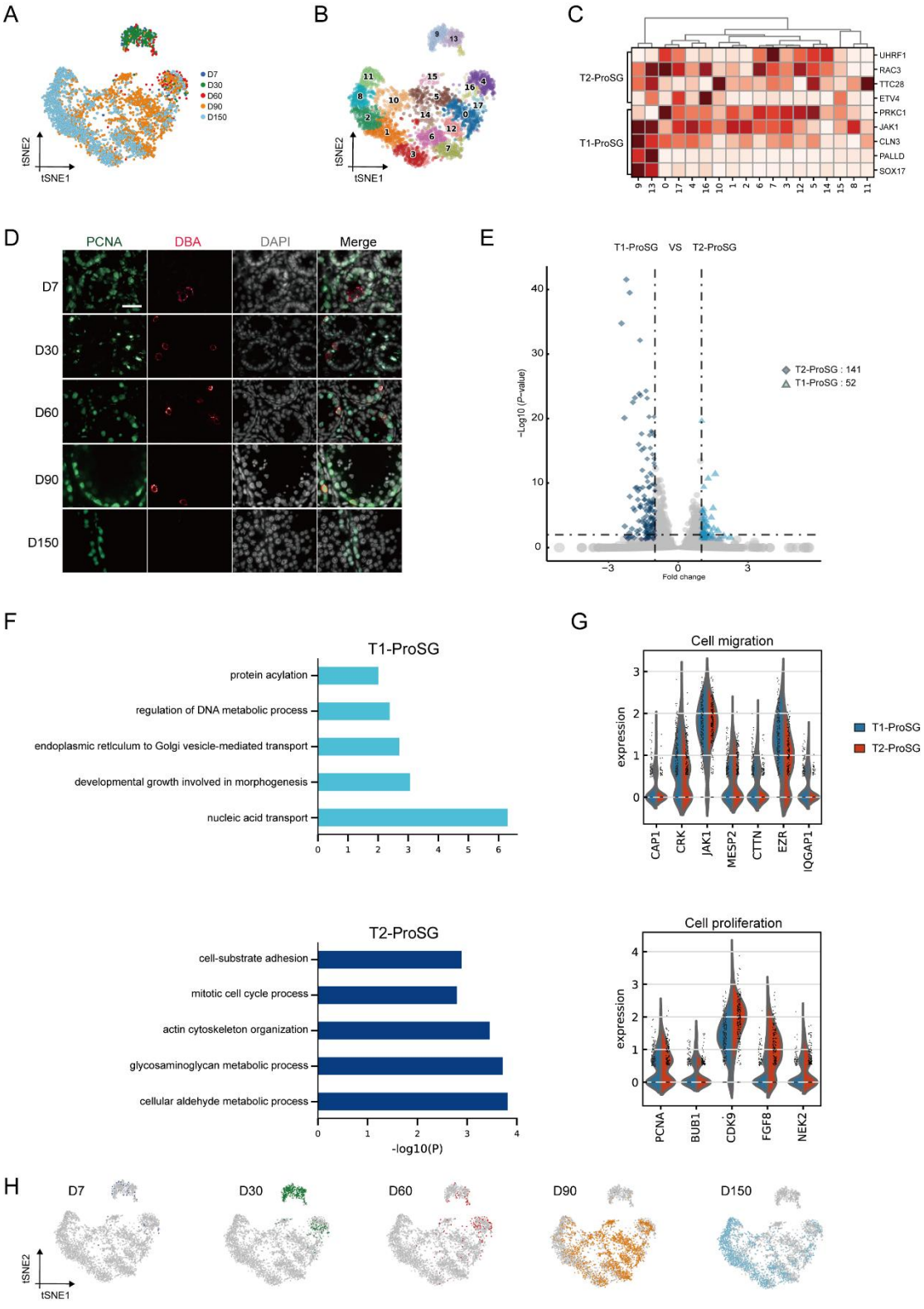

Supplementary Figure S2 Distinct phases of proliferation and migration in ProSG during porcine puberty. A: Focused analysis (t-SNE and clustering) of ProSG and spermatogonia showing developmental progression during puberty. Cells are colored based on ages. B: t-SNE plot showing unbiased Leiden clusters from ProSG and spermatogonia. C: Heatmap showing expression of T1-ProSG and

T2-ProSG marker genes in unbiased cell clusters. Differential gene expression levels are based on Z scores, as defined by color key. D: Immunolocalization co-staining of PCNA and DBA at different ages (7–150 days old), showing ProSG disappeared around D90. Scale bar=50 μm. E: Volcano plot showing differentially expressed genes (DEGs) between T1-ProSG (n=52) and T2-ProSG (n=141). F: Enrichment terms and *P*-values for DEGs of T1-ProSG and T2-ProSG. G: Violin plot showing expression of genes associated with cell migration and proliferation in both T1-ProSG and T2-ProSG. H: Deconvolution of cell distribution plot according to ages/individuals.

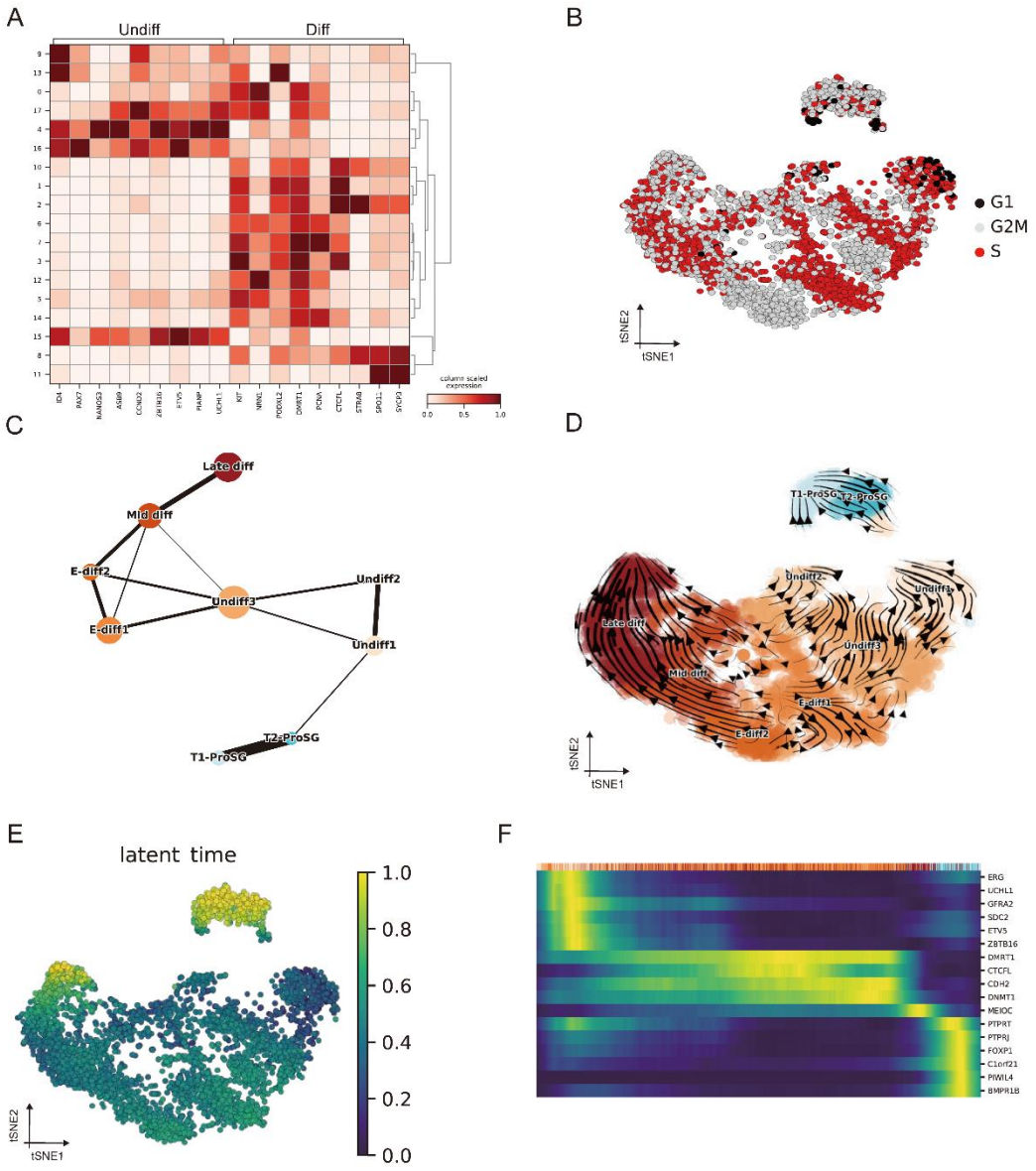

Supplementary Figure S3 Single-cell porcine spermatogonia trajectories reveal transitions with differentiation. A: Heatmap showing expression of undifferentiated and differentiated spermatogonia marker genes in Leiden cell clusters. B: Annotation of cell cycle score and cell cycle phase for ProSG and spermatogonia in t-SNE plots (G1-phase, black; S-phase, red; G2M, gray). C: PAGA graph showing ProSG and spermatogonia clusters. Size of clusters is proportional to cell number, and thickness of lines between clusters is proportional to connection strength. D: t-SNE plot showing *scVelo*-derived dynamics in ProSG and spermatogonia clusters. E: Single-cell transcriptomes of ProSG and spermatogonia were used for cell trajectories, ordered in latent time. F: Heatmap showing variable genes across latent time from identified cell types of ProSG and spermatogonia.

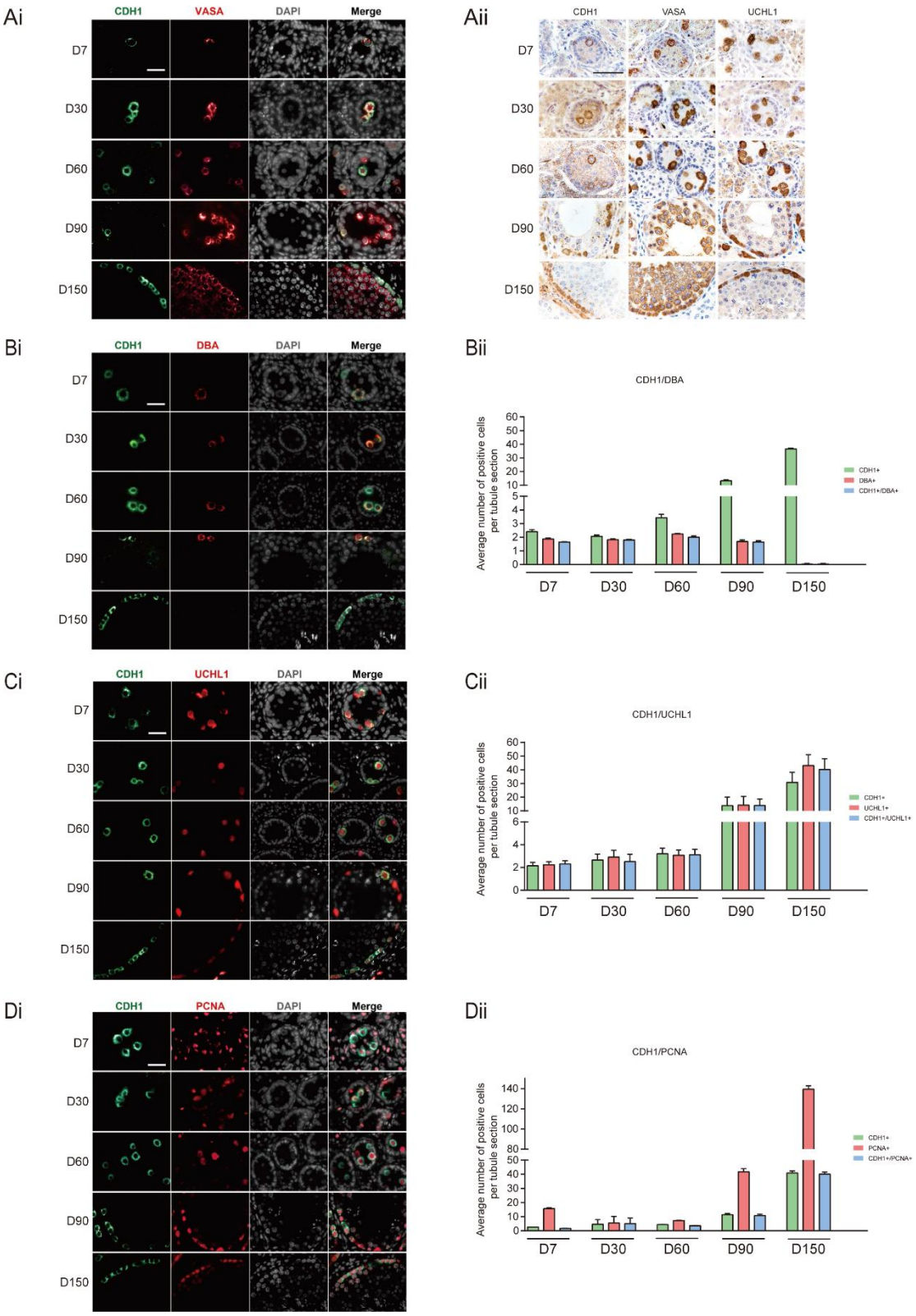

Supplementary Figure S4 Expression of CDH1 in porcine testes at different ages. Ai: Co-immunofluorescence of CDH1 and VASA expression. Scale bars=50 μm. Aii: Immunohistochemical staining of CDH1, VASA, and UCHL1 during porcine testicular development. Scale bars=50 μm. Bi: Immunolocalization co-staining of CDH1 and DBA. Scale bar=50 μm. Bii: Average number of $CDH1^{+}$, DBA^{+}, and

$CDH1^+/DBA^+$ germ cells per tubule in porcine testes at different ages. Data are mean±SD of three independent experiments. Ci: Immunolocalization co-staining of CDH1 and UCHL1. Scale bar=50 μm. Cii: Average number of $CDH1^+$, $UCHL1^+$, and $CDH1^+/UCHL1^+$ germ cells per tubule in porcine testes at different ages. Data are mean±SD of three independent experiments. Di: Co-immunofluorescence of CDH1 and PCNA expression. Scale bars=50 μm. Dii: Average number of $CDH1^+$, $PCNA^+$, and $CDH1^+/PCNA^+$ germ cells per tubule in porcine testes at different ages. Data are mean±SD of three independent experiments.

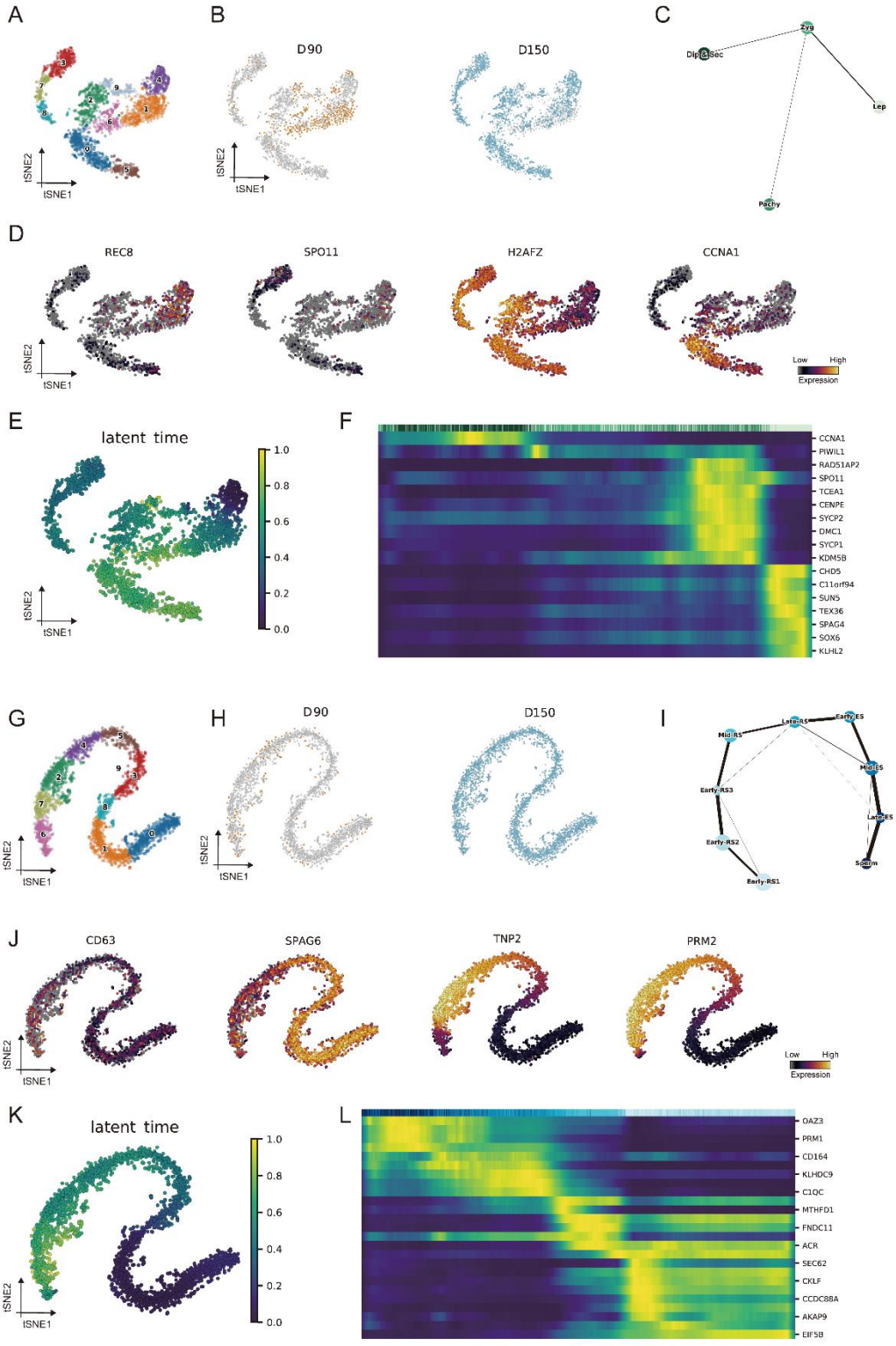

Supplementary Figure S5 Identification of spermatocyte and spermatid subtypes during puberty. A: t-SNE plot showing unbiased cell clusters from spermatocytes. B: t-SNE plot showing distribution of spermatocytes at D90 and D150. C: PAGA graph showing spermatocyte clusters. D: Visualization of selected spermatocyte marker gene expression levels across all single cells in t-SNE plot. E: Single-cell transcriptomes from spermatocytes were used for cell trajectories, ordered in latent

time. F: Heatmap showing variable genes across latent time from identified spermatocyte cell types. G: t-SNE plot showing unbiased cell clusters from spermatids. H: t-SNE plot showing distribution of spermatids at D90 and D150. I: PAGA graph showing spermatid clusters. J: Visualization of selected spermatid marker gene expression levels across all single cells in t-SNE plot. K: Single-cell transcriptomes from spermatids were used for cell trajectories, ordered in latent time. L: Heatmap showing variable genes across latent time from identified spermatid cell types.

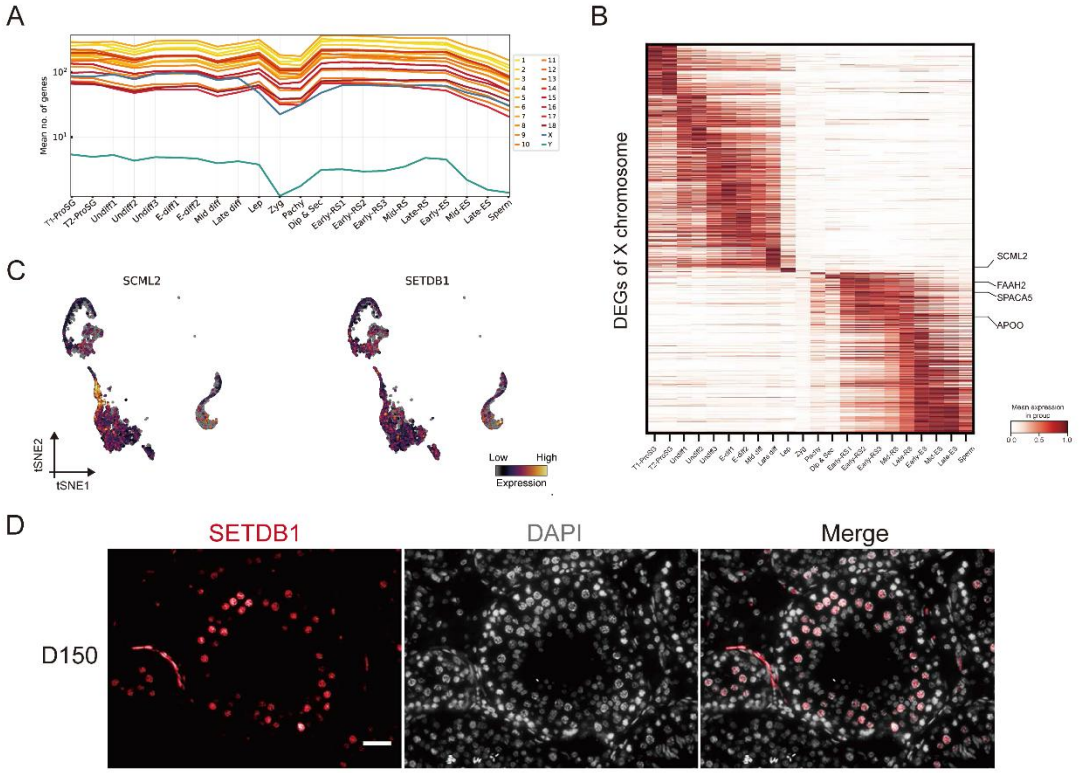

Supplementary Figure S6 X chromosome dynamics during porcine spermatogenesis. A: Line plot showing mean number of genes expressed from every chromosome in each cell type during porcine spermatogenesis. (Chromosomes are colored according to legend) B: Heatmap showing all expressed genes on pig X chromosome during spermatogenesis. C: t-SNE plot showing gene expression of SCML2 and SETDB1. D: Immunofluorescence staining of SETDB1 in porcine testis, suggesting SETDB1 plays a critical role in porcine meiosis. Scale bars=50 μm.

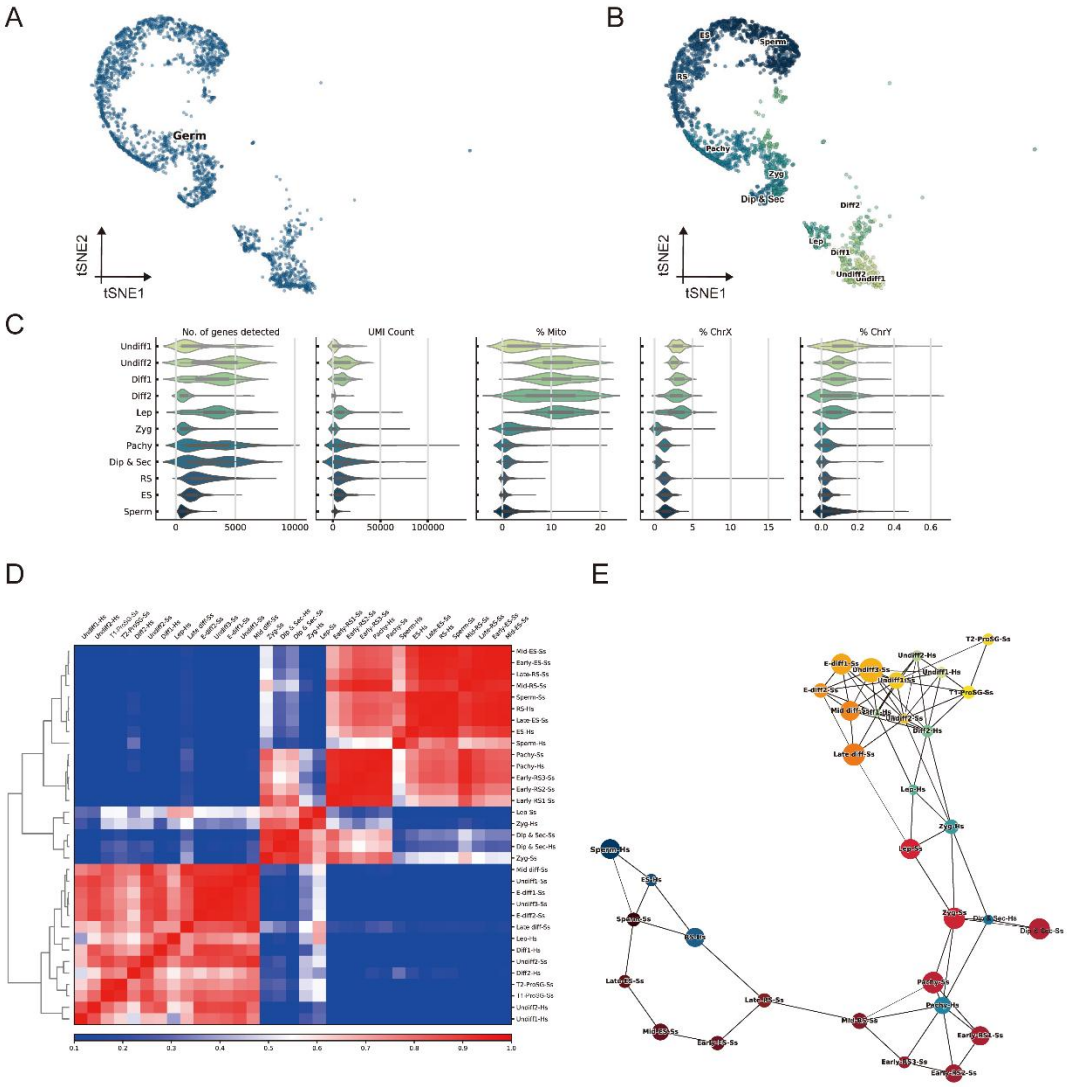

Supplementary Figure S7 Comparative analysis of germ cells in pigs and humans. A: t-SNE plot showing distribution of germ cells in human datasets. B: t-SNE plot showing identified germ cell types in humans (colored by 11 cell types, i.e., Undiff1, Undiff2, Diff1, Diff2, Lep, Zyg, Pachy, Dip & Sec, RS, ES, and Sperm). C: Distribution of cell attributes from each cell type in human datasets. D: Correlation analysis and hierarchical clustering of germ cell clusters across two species. E: PAGA graph of cluster relationships from integrated dataset.